MUC4 Mucin Potentiates Pancreatic Tumor Cell Proliferation, Survival, and Invasive Properties and Interferes with Its Interaction to Extracellular Matrix Proteins

Pallavi Chaturvedi,[1] Ajay P. Singh,[1] Nicolas Moniaux,[1] Shantibhushan Senapati,[1] Subhankar Chakraborty,[1] Jane L. Meza,[3] and Surinder K. Batra[1,2]

[1]Department of Biochemistry and Molecular Biology, [2]Eppley Institute for Research in Cancer, and [3]Department of Societal and Preventive Medicine, University of Nebraska Medical Center, Omaha, Nebraska

Abstract

MUC4, a transmembrane mucin, is aberrantly expressed in pancreatic adenocarcinomas while remaining undetectable in the normal pancreas. Recent studies have shown that the expression of *MUC4* is associated with the progression of pancreatic cancer and is inversely correlated with the prognosis of pancreatic cancer patients. In the present study, we have examined the phenotypic and molecular consequences of *MUC4* silencing with an aim of establishing the mechanistic basis for its observed role in the pathogenesis of pancreatic cancer. The silencing of *MUC4* expression was achieved by stable expression of a *MUC4*-specific short hairpin RNA in CD18/HPAF, a highly metastatic pancreatic adenocarcinoma cell line. A significant decrease in *MUC4* expression was detected in *MUC4*-knockdown (CD18/HPAF-siMUC4) cells compared with the parental and scrambled short interfering RNA–transfected (CD18/HPAF-Scr) control cells by immunoblot analysis and immunofluorescence confocal microscopy. Consistent with our previous observation, inhibition of *MUC4* expression restrained the pancreatic tumor cell growth and metastasis as shown in an orthotopic mouse model. Our *in vitro* studies revealed that MUC4-associated increase in tumor cell growth resulted from both the enhanced proliferation and reduced cell death. Furthermore, *MUC4* expression was also associated with significantly increased invasiveness ($P \leq 0.05$) and changes in actin organization. The presence of MUC4 on the cell surface was shown to interfere with the tumor cell-extracellular matrix interactions, in part, by inhibiting the integrin-mediated cell adhesion. An altered expression of growth- and metastasis-associated genes (*LI-cadherin, CEACAM6, RAC1, AnnexinA1, thrombomodulin, epiregulin, S100A4, TP53, TP53BP, caspase-2, caspase-3, caspase-7, plakoglobin*, and *neuregulin-2*) was also observed as a consequence of the silencing of *MUC4*. In conclusion, our study provides experimental evidence that supports the functional significance of MUC4 in pancreatic cancer progression and indicates a novel role for MUC4 in cancer cell signaling. (Mol Cancer Res 2007;5(4):309–20)

Introduction

Mucins are heavily glycosylated proteins that establish a selective molecular barrier at the epithelial surface and engage in signal transduction pathways that regulate morphogenesis (1, 2). In addition, mucins influence many cellular processes, including growth, differentiation, transformation, adhesion, invasion, and immune surveillance (1, 3). Previous studies have shown that MUC4, a transmembrane mucin, is expressed by epithelial cells in a variety of tissues (3-5). In the pancreas, however, *MUC4* is not expressed under normal conditions, although its aberrant expression is reported in premalignant and malignant pancreatic lesions as well as in several pancreatic cancer cell lines (3, 6-10). Recent studies from our laboratory and elsewhere have indicated a strong association between *MUC4* overexpression and pancreatic carcinogenesis, thereby implicating MUC4 as a novel target for diagnosis, prognosis, and therapy (3, 6-12).

MUC4 is a high-molecular-weight glycoprotein with multidomain organization (13-15). The deduced full-length amino acid sequence of the MUC4 apoprotein shows the presence of a leader peptide, a serine and threonine rich nontandem repeat region, central large tandem repeat domain containing 16-amino acid repetitive units, regions rich in potential N-glycosylation sites, two cysteine-rich domains, a putative GDPH proteolytic cleavage site, three epidermal growth factor–like domains, a hydrophobic transmembrane domain, and a short cytoplasmic tail. MUC4 mucin shares many structural similarities with the sialomucin complex (SMC/ratMuc4), which has previously been shown to facilitate

Received 10/18/06; revised 1/30/07; accepted 2/2/07.
Grant support: NIH grant CA 78590.
The costs of publication of this article were defrayed in part by the payment of page charges. This article must therefore be hereby marked *advertisement* in accordance with 18 U.S.C. Section 1734 solely to indicate this fact.
Note: Supplementary data for this article are available at Molecular Cancer Research Online (http://mcr.aacrjournals.org/).
Requests for reprints: Surinder K. Batra, Department of Biochemistry and Molecular Biology, Eppley Institute for Research in Cancer and Allied Diseases, University of Nebraska Medical Center, 985870 Nebraska Medical Center, Omaha, NE 68198-5870. Phone: 402-559-5455; Fax: 402-559-6650. E-mail: sbatra@unmc.edu

doi:10.1158/1541-7786.MCR-06-0353

tumor progression by multiple mechanisms (3, 13, 16-19). SMC/Muc4 is a heterodimeric glycoprotein composed of an *O*-glycosylated mucin subunit, ascites sialoglycoprotein-1, and an *N*-glycosylated transmembrane subunit, ascites sialoglycoprotein-2. Similarly, MUC4 also possesses two subunits: an extracellular mucin-like subunit, MUC4α, and a growth factor–like transmembrane subunit, MUC4β, containing three epidermal growth factor–like domains (3). The SMC/Muc4 is known to act as an intramembrane ligand for the receptor tyrosine kinase ErbB2/HER2/neu, inducing its limited phosphorylation via one of the epidermal growth factor domains (17, 20, 21). On the other hand, a recent study from our laboratory has indicated that MUC4 may modulate HER2 signaling by regulating its expression (11).

In the present study, we have elucidated the multiple roles of MUC4 in pancreatic cancer progression. The silencing of *MUC4* was achieved by stable expression of a MUC4-specific short hairpin RNA (shRNA) in a *MUC4*-overexpressing (CD18/HPAF) pancreatic cancer cell line. The functional association of *MUC4* expression with cancer phenotype was determined in various *in vitro* and *in vivo* studies. Our results show that the overexpression of *MUC4* is associated with increased tumor cell proliferation, survival, invasiveness, and metastasis. Moreover, MUC4 interferes with the interaction between tumor cell and extracellular matrix (ECM) proteins, in part, by blocking the accessibility of integrins to ECM ligands. Furthermore, an altered expression of growth- and metastasis-associated genes is also reported on *MUC4* down-regulation, indicating a novel role for MUC4 in cancer cell signaling.

Results

Short Interfering RNA–Mediated Silencing of MUC4 Expression Inhibits Tumorigenicity and Metastasis of CD18/HPAF Pancreatic Cancer Cells

CD18/HPAF cells were transduced with the viral supernatant carrying either the MUC4 shRNA or the scrambled shRNA expression plasmids for effective silencing of *MUC4* or to serve as control, respectively. The stable clones were selected in medium containing puromycin (3.0 μg/mL) and expanded, and the expression of *MUC4* was examined by immunoblotting. All the clones ($n = 19$) selected from MUC4 short interfering RNA (siRNA)-transfected CD18/HPAF cells showed a 20% to 90% down-regulation of *MUC4* (data not shown). Three clones (clones 9, 10, and 12) that consistently showed >70% reduced expression of *MUC4* were pooled (CD18/HPAF-siMUC4) to avoid clonal variation in further investigations. The stable silencing of *MUC4* in CD18/HPAF-siMUC4 cells compared with mixed population of scrambled shRNA-transfected cells (CD18/HPAF-Scr) was monitored by immunoblot and confocal microscopic analyses (Fig. 1A and B). Western blot analysis

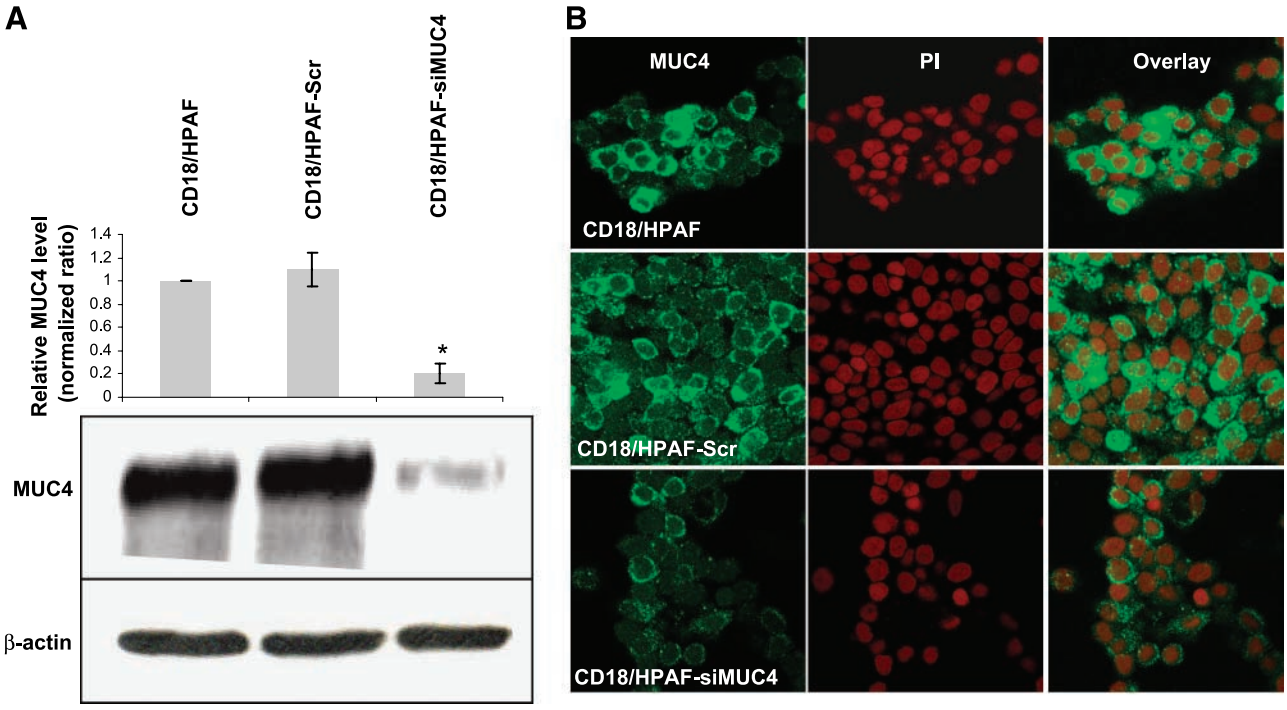

FIGURE 1. Analyses of MUC4 expression in CD18/HPAF and its derived sublines: CD18/HPAF-Scr (mixed population of scrambled shRNA-transfected cells) and CD18/HPAF-siMUC4 (pooled population of MUC4 shRNA-transfected cells). **A.** Western blot analysis; a total of 10 μg protein from cell extracts was resolved by electrophoresis on a 2% SDS-agarose (for MUC4) and 10% SDS-polyacrylamide gel (for β-actin), transferred to polyvinylidene difluoride membrane, and incubated with anti-MUC4 or anti-β-actin monoclonal antibody. The membrane was then probed with horseradish peroxidase–labeled goat anti-mouse immunoglobulin, and the signal was detected using an electrochemiluminescence reagent kit. The intensity of signals was quantified by densitometry. β-Actin was used as an internal control. Columns, mean normalized fold difference in MUC4 protein expression levels ($n = 3$); bars, SE. *, $P < 0.05$. **B.** Expression analysis of MUC4 using confocal microscopy. CD18/HPAF, CD18/HPAF-Scr, and CD18/HPAF-siMUC4 cells were grown at low density on sterilized coverslips, washed, and fixed in ice-cold methanol at −20°C. The cells were blocked in 10% goat serum and incubated with the anti-MUC4 mouse monoclonal antibody. After washing, the cells were incubated with FITC-conjugated goat anti-mouse IgG. Cells were mounted on glass slides in antifade Vectashield mounting medium before observation under a Zeiss confocal laser-scanning microscope. Magnification, ×630. PI, propidium iodide.

showed ~80% (on an average) down-regulation of *MUC4* expression in CD18/HPAF-siMUC4 compared with control cells. Results of the confocal immunofluorescence microscopy were also consistent with the Western blot analysis, further confirming the reduced cellular expression of *MUC4* in CD18/HPAF-siMUC4 cells compared with control cells. Additionally, we also examined the expression of *MUC4* at transcript level by real-time reverse transcription-PCR and the results were in support with that obtained by immunoblot analysis (Supplementary Fig. S1).

The derived heterogeneous populations were studied to observe the effect of *MUC4* silencing on tumor cell growth and metastasis in immunodeficient mice. All the mice injected orthotopically with the CD18/HPAF-Scr or CD18/HPAF-siMUC4 cells developed primary tumors. The tumor weight and volume were significantly lower ($P = 0.02$ and $P < 0.001$, respectively) in mice injected with the *MUC4*-knockdown (CD18/HPAF-siMUC4) cells compared with those injected with control (CD18/HPAF-Scr) cells. The mean weight and volume were 1,390.07 mg and 0.986 cm^3 for the tumors developed from CD18/HPAF-Scr cells and 864.62 mg and 0.437 cm^3 for those produced from the CD18/HPAF-siMUC4 cells, respectively (Supplementary Fig. S2A and B). The incidence of metastases to distant organ sites was also reported (Supplementary Table S1). All the mice injected with the CD18/HPAF-Scr cells developed metastases to one or multiple sites, whereas only 29% (4 of 14) of the mice injected with the *MUC4*-knockdown cells had detectable metastases. The most common sites of metastases were the lymph nodes, liver, and lungs. Specifically, the incidence of lymph node and liver metastases was lower in the mice injected with the *MUC4*-knockdown cells compared with those injected with the control cells (Supplementary Table S1). Immunohistochemical analysis of the primary tumor tissue sections was done with the anti-MUC4 mouse monoclonal antibody to monitor the expression of MUC4. Staining confirmed the down-regulated expression of *MUC4* in tumors developed from CD18/HPAF-siMUC4 cells (Supplementary Fig. S3).

MUC4-Associated Increase in Tumor Cell Growth Results from Enhanced Proliferation and Reduced Apoptosis of Pancreatic Cancer Cells

The siRNA-induced silencing of *MUC4* in CD18/HPAF pancreatic cancer cells led to the suppression of both the tumor growth and metastasis. These results were consistent with our previous observation in which *MUC4* expression was down-regulated by antisense technology (11). A reduced growth rate was also observed in the *MUC4*-knockdown cells *in vitro* (data not shown). Because the overall rate of cell growth is determined by the balance between cell proliferation and apoptosis, we next determined the proliferation and apoptotic indices of the CD18/HPAF-Scr and CD18/HPAF-siMUC4 pancreatic cancer cells. The proliferation index was determined by first synchronizing the cells at the G_1-S boundary using a double thymidine block followed by propidium iodide staining and flow cytometry (Fig. 2). The total percentage of CD18/HPAF-Scr cells that entered into the S phase was 42.51% compared with 17.71% in CD18/HPAF-siMUC4 cells, indicating

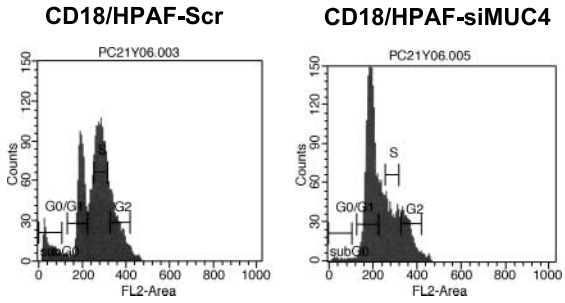

Cell cycle analyses: per cent of cells in each stage of cell cycle

Cell cycle stage	CD18/HPAF-Scr	CD18/HPAF-siMUC4
G0/G1	**22.74**	**55.48**
S	**42.51**	**17.17**
G2	**15.13**	**12.77**

FIGURE 2. Cell cycle analysis of *MUC4*-knockdown cells compared with control cells. CD18/HPAF cells, either knocked down for MUC4 expression or transfected with scrambled shRNA expression construct, were synchronized with double thymidine block. Following synchronization, cells were stained with propidium iodide and analyzed by fluorescence-activated cell sorting to evaluate the number of cells in different stages of cell cycles.

a higher rate of proliferation in the *MUC4*-overexpressing (CD18/HPAF-Scr) cells.

To analyze the apoptotic index, the *MUC4*-overexpressing and MUC4-silenced cells were serum starved and the extent of apoptosis and necrosis was determined by Annexin V and propidium iodide staining, respectively, followed by flow cytometry. The apoptotic index in CD18/HPAF-siMUC4 cells was nearly double to that reported for CD18/HPAF-Scr cells, whereas no changes in the necrosis were reported (Fig. 3). Taken together, our data show that MUC4 enhances cell proliferation and favors the cell survival in CD18/HPAF pancreatic cancer cells.

Silencing of MUC4 Expression Decreases Cell Motility and Invasiveness of Pancreatic Cancer Cells and Induces Actin Reorganization

The aggressiveness of a malignant cell is determined by its potential to invade the ECM and metastasize to distant sites. Several studies have supported the idea that the invasive and metastatic potential of cancer cells is intimately related to their motility (22). As the *MUC4*-overexpressing cells were more metastatic than the *MUC4*-knockdown cells, we examined if the expression of *MUC4* is associated with enhanced motility of the CD18/HPAF pancreatic cancer cells. Consistent to our previous observation (11), *MUC4*-knockdown (CD18/HPAF-siMUC4) cells showed a significant decrease ($P < 0.001$) in motility (~5-fold) compared with the control (CD18/HPAF-Scr) cells (Fig. 4A). To further examine if the increased cell motility also correlated with the invasive potential of pancreatic cancer cells, we did an *in vitro* Matrigel invasion assay. We observed that nearly one third of the *MUC4*-knockdown (CD18/HPAF-siMUC4) cells invaded the Matrigel when compared with control (CD18/HPAF-Scr) cells (Fig. 4B).

Given the key role played by the actin in defining cell shape and in orchestrating events related to cell movement (23), we

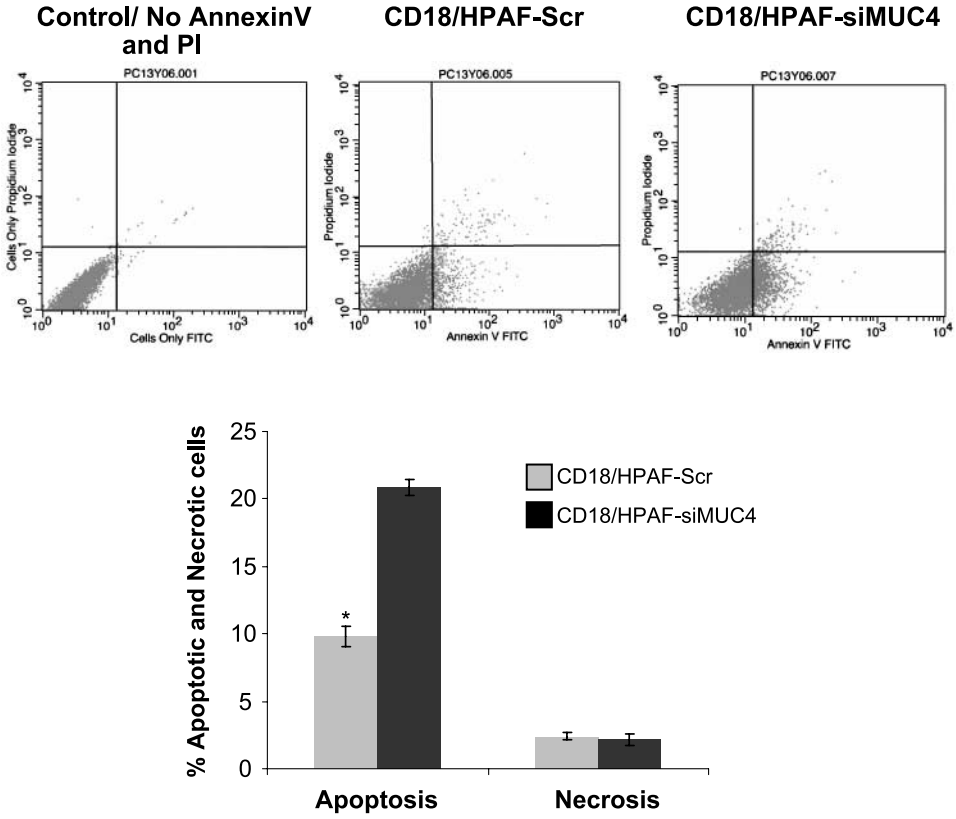

FIGURE 3. Analysis of apoptotic index of MUC4-knockdown cells compared with control cells. CD18/HPAF cells, either knocked down for *MUC4* expression or transfected with scrambled shRNA expression construct, were serum starved to induce apoptosis. The percentage of cells undergoing apoptosis or necrosis was measured by Annexin V and propidium iodide staining, respectively, followed by fluorescence-activated cell sorting analysis. Bottom left quadrant, being negative for both Annexin V and propidium iodide, shows the live cells; bottom right quadrant, being Annexin V positive and propidium iodide negative, shows the early apoptotic cells; top right quadrant, being both propidium iodide positive and Annexin V positive, shows the late apoptotic or necrotic cells. Columns, mean percentage of the apoptotic and necrotic cells ($n = 3$). *, $P < 0.05$.

next chose to focus our attention on the effect of *MUC4* expression in reorganization of the actin cytoskeleton. In a highly motile cell, the actin filaments are organized on the mobile protruding edges, called lamellipodia, and can be visualized by confocal microscopy after staining with fluorescent dye-tagged phalloidin. Phalloidin is a fungal toxin that binds to filamentous actin and prevents its depolymerization into G-actin monomers (24). The staining of the control (CD18/HPAF-Scr) and *MUC4*-knockdown (CD18/HPAF-siMUC4) cells with Alexa Fluor 488–conjugated phalloidin showed the presence of many lamellipodial structures in the control cells, although they were less obvious in the *MUC4* down-regulated cells (Fig. 4C). This suggests that the expression of *MUC4* induces actin reorganization, thereby facilitating the motility and, in turn, the invasiveness of pancreatic cancer cells.

MUC4 Alters the Interaction of Pancreatic Tumor Cells with the ECM Components, in Part, by Interfering with the Accessibility of Integrins

Another important role envisaged for MUC4 is that of a modulator of cell-cell and cell-ECM interactions (16). In a previous study, we showed that MUC4 altered the cell-cell aggregation and cell adhesion on a plastic surface (11). To further study the role played by MUC4 in tumor cell-ECM interactions, CD18/HPAF-Scr and CD18/HPAF-siMUC4 cells were compared for their binding affinity to various ECM components (laminin I, collagen I, collagen IV, fibronectin, and basement matrix complex). The *MUC4*-knockdown cells showed significantly higher ($P < 0.05$) binding to laminin, basement matrix complex, collagen IV, collagen I, and fibronectin compared with the CD18/HPAF-Scr cells (Fig. 5). These results suggest that the overexpression of *MUC4* in pancreatic tumors reduces the ability of tumor cell to interact with ECM proteins.

Integrins are the cell surface receptors for the ECM proteins (25). Given the observation that overexpression of *MUC4* decreases adherence of tumor cell to ECM components, we decided to investigate the possible relationship between decreased adhesiveness and integrin expression in *MUC4*-overexpressing versus *MUC4*-knockdown cells. CD18/HPAF-Scr and CD18/HPAF-siMUC4 cells were seeded on anti-integrin-coated ($\alpha2$, $\alpha3$, and $\alpha5$) plates and allowed to adhere for 1.0 h. A significantly reduced adhesion ($P < 0.05$) of the CD18/HPAF-Scr cells to the anti-integrin-coated plates was observed compared with the CD18/HPAF-siMUC4 cells (Fig. 6A). Analysis of $\alpha2$, $\alpha3$, and $\alpha5$ integrins by immunoblot assay, however, did not reveal any changes in their expression between *MUC4*-overexpressing and *MUC4*-knockdown cells (data not shown), which suggested a direct involvement of MUC4 in interfering with the accessibility of integrins to their coated antibodies. To obtain the evidence that cell surface expression of *MUC4* inhibits the integrin-mediated adhesion, the cells were incubated with FITC-labeled monoclonal antibody (8G7) raised against the tandem repeat peptide of *MUC4*. Due to repetitive nature of epitope, the antibody binding leads to the clustering of the cell surface MUC4 molecules in multiple patches or in the form of a cap (Fig. 6B). The MUC4 clustering at the cell surface enhanced the adhesion

of CD18/HPAF-Scr cells on the anti-integrin antibody-coated plates, although it had no significant effect on the binding of CD18/HPAF-siMUC4 cells (Fig. 6C). Furthermore, no changes in the adhesion were observed when cells were incubated with a nonspecific antibody (keyhole limpet hemocyanin antibody; data not shown). These observations suggest that MUC4 interferes with the accessibility of integrins to its ligands by causing the steric hindrance at the cell surface.

MUC4 Enhances the Expression of Growth- and Metastasis-Associated Genes

DNA oligonucleotide microarrays representing ~12,000 genes were used to identify genes regulated by MUC4 and potentially responsible for differences in the metastatic properties of *MUC4*-knockdown cells. The mRNA expression profile of CD18/HPAF-siMUC4 cells was compared with that of CD18/HPAF-Scr cells. A total of 173 genes was found to be differentially expressed in cells where *MUC4* expression had been silenced. Of these, a few selected genes that were down-regulated or overexpressed in the *MUC4*-knockdown cells are listed in Tables 1 and 2, respectively. Analysis of the data revealed that several growth- and metastasis-associated genes were down-regulated in the *MUC4*-knockdown cells. Of particular importance were the genes encoding LI-cadherin, CEACAM6, S100A4, tumor-associated calcium signal transducer-2, macrophage inhibitory cytokine 1, AnnexinA1, RAC1, epiregulin, and neuregulin-2 (Table 1). Among the genes that were up-regulated in *MUC4*-knockdown cells were those encoding for somatostatin, seladin-1, TP53, TP53BP, caspase-2, caspase-3, caspase-7, desmoglein-2, plakoglobin, and SMAC1. To validate our microarray data, expression of few differentially expressed genes was examined by Western blot analysis (Fig. 7). The results of the Western blot analysis were in complete agreement with the microarray data, indicating that these could be functionally implicated in mediating the MUC4- modulated metastatic pathways.

Discussion

Our previous studies have implicated MUC4 mucin as an important player in the pathogenesis of pancreatic cancer (6, 7, 11, 12). In the present work, we provide additional evidence to buttress our earlier findings and provide mechanistic basis for the role of MUC4 in pancreatic cancer progression. We show

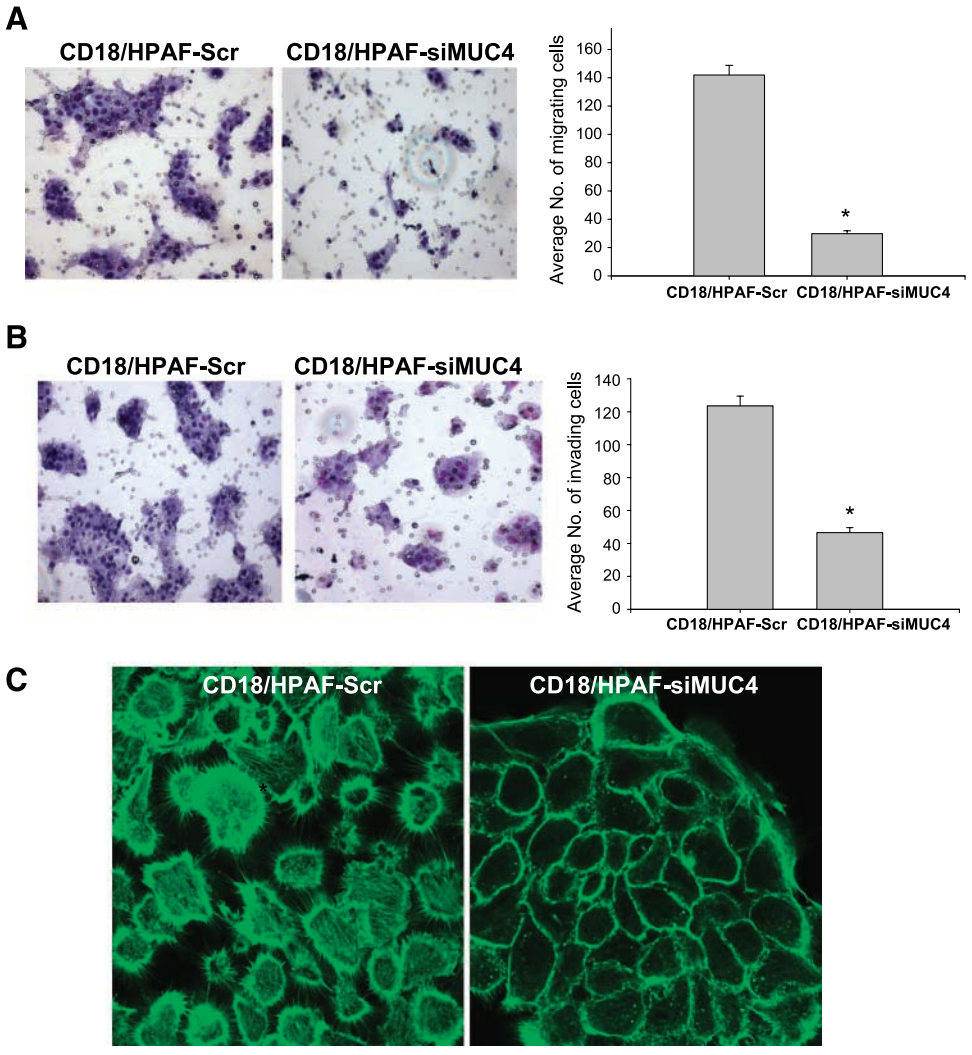

FIGURE 4. Effect of *MUC4* down-regulation on cell motility and invasion. Cells were plated on noncoated or Matrigel-coated membranes for motility (**A**) and invasion (**B**) assays, respectively, and incubated for 24 h. Medium containing 10% fetal bovine serum in the lower chamber was used as a chemoattractant. The cells that did not migrate through the Matrigel and/or pores in the membrane were removed, and cells on the other side of the membrane were stained and photographed under bright-field microscopy. Magnification, ×100. The number of cells migrated through the membrane was determined by averaging 10 random fields of view. Data are the number of cells per field of view. Columns, average of three independent experiments; bars, SE. *, $P < 0.05$. **C.** Actin organization. The MUC4-knockdown and control cells were grown on coverslips, fixed with 4% paraformaldehyde in PBS, permeabilized with 0.2% Triton X-100 in PBS for 5 min, and stained with Alexa Fluor 488–conjugated phalloidin. Increased lamellipodial structures were observed in parental and control-transfected CD18/HPAF cells compared with the MUC4-knockdown cells.

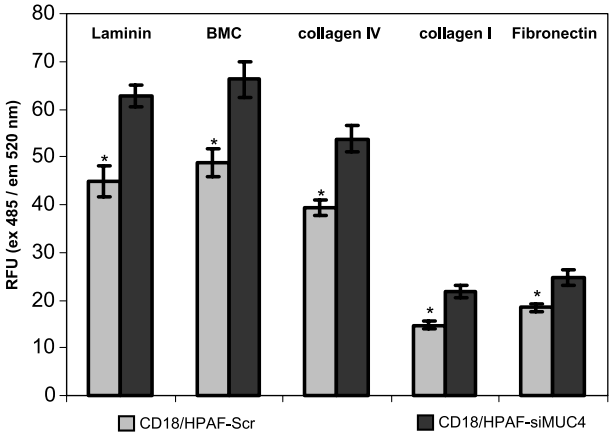

FIGURE 5. Cell adhesion assay. Cells (25×10^3) were seeded in 96-well plate coated separately with laminin, collagen I, fibronectin, collagen IV, and basement membrane protein complex (*BMC*) proteins. Wells coated with bovine serum albumin and poly-L-lysine served as negative and positive controls, respectively. The cells were allowed to adhere for 1 h at 37°C, washed twice with PBS, and labeled with calcein-AM dye for 1 h at 37°C. The fluorescence of adhered cells was measured at an emission wavelength of 520 nm after excitation at 485 nm. The fluorescent intensity obtained in the negative control (bovine serum albumin–coated wells) was subtracted from the values obtained for different treatments (ECM component-coated wells). After that, a relative fluorescence unit (*RFU*) was calculated for all treatments with respect to the intensity value obtained with the positive control (poly-L-lysine–coated plates; $n = 3$). *, $P < 0.05$.

here that siRNA-mediated silencing of *MUC4* restrains growth and metastasis of CD18/HPAF pancreatic adenocarcinoma cells. Our *in vitro* studies show that the increase in tumor cell growth associated with *MUC4* overexpression results from enhanced proliferation and reduced cell death. *MUC4* expression is also associated with actin reorganization and cancer cell invasiveness. Moreover, the presence of MUC4 on the cell surface interferes with the tumor cell-ECM interaction, in part, by inhibiting integrin-mediated cell adhesion. Further, *MUC4* down-regulation was found to alter the expression of several growth- and metastasis-associated genes.

Normal cell growth is maintained by the balance between cell proliferation and cell death. While studying the cause for the reduced tumor growth in *MUC4*-knockdown cells, we observed that an increase in *MUC4* expression is associated with a higher rate of cell proliferation and reduced apoptosis (Figs. 2 and 3). In a previous study, the overexpression of SMC/Muc4 (the rat homologue of MUC4) was reported to accelerate the growth of xenotransplanted A375 melanoma cells in host animals by suppressing the apoptosis (18). Muc4 was shown to act as an intramembrane ligand for ErbB2/HER2/neu, inducing its limited phosphorylation. It was also suggested that Muc4-induced ErbB2/neu signaling might mediate the antiapoptotic function of Muc4 (18). Consistent with our previous report (11), we also observed a down-regulation of the receptor tyrosine kinase, HER2, and its downstream signaling in *MUC4*-knockdown pancreatic cancer cells (data not shown). A down-regulation of growth-promoting genes and an up-regulation of apoptosis-inducing genes were also observed in CD18/HPAF-siMUC4 cells (Tables 1 and 2). This may explain the changes in the pancreatic cancer cell growth in response to *MUC4* silencing. Particularly, MUC4-mediated down-regulation of tumor suppressors, such as *TP53* and *TP53BP1*, might aid the *MUC4*-expressing tumor cells in surpassing the cell cycle checkpoints and, thus, facilitate their uncontrolled cell growth (26). Moreover, the down-regulation of apoptosis mediators (*caspase-2, caspase-3, caspase-7, TP53I11,* and *SMAC*; refs. 27-29) in *MUC4*-overexpressing control cells might lead to enhanced cell survival.

Apart from increased tumorigenicity, *MUC4*-expressing cells also showed an enhanced tendency to metastasize to distant organs. The process of metastasis is a complex phenomenon regulated by many components, which work in tandem to facilitate the detachment of tumor cells from their site of origin and subsequent spread to secondary sites (30). Similar to our previous observations (11), the *MUC4* down-regulated cells showed a significant decrease in motility (Fig. 4). Furthermore, our present study showed that *MUC4*-knockdown cells were less invasive compared with the control cells (Fig. 4B). Cell motility and invasiveness are typically associated with the actin reorganization (23). In a highly motile cell, the actin is organized on the mobile protruding edges called lamellipodia (23). An increase in lamellipodia-like structures was observed in the *MUC4*-expressing cells, although these structures were less obvious in the knockdown cells (Fig. 4C). Thus, our findings lend support to the novel idea that MUC4 induces remodeling of the actin cytoskeleton and thereby contributes to enhanced cell motility and invasiveness. The molecular basis of MUC4-induced changes in actin organization is yet to be investigated. Cell-cell interactions, including cadherin-mediated interactions, restrict cell motility (31). Steric hindrance caused by the large extracellular domain of MUC4 may disrupt these interactions (11) and might indirectly be responsible for rearrangements in the actin cytoskeleton and, hence, enhanced motility. Alternatively, as discussed later, *MUC4* expression might affect multiple signaling pathways either by affecting the ligand accessibility to their corresponding receptors or by directly interacting with the signal transducers, leading to transcriptional or posttranscriptional activation of the regulators of cell motility. Therefore, it can be suggested that MUC4 influences the cancer cell signaling in favor of the metastatic behavior of the tumor cells.

Another important finding of this study was the enhanced tumor cell-ECM interaction on abrogation of *MUC4* expression (Fig. 5). An antiadhesive property of transmembrane mucins is predicted due to the presence of a highly glycosylated tandem repeat domain, which may sterically hinder their homotypic and heterotypic interactions (1). Our results showed that adhesion of pancreatic tumor cells to laminin, collagen IV, collagen I, and fibronectin and basement membrane proteins was significantly increased in *MUC4* down-regulated cells (Fig. 5). The interaction of the cell with the ECM components is mediated by a family of cell surface receptors, integrins. Till date, more than 20 different integrins and several additional splice variants have been identified, with a specific subset being expressed by each cell type (25, 32). MUC4 masked the surface epitopes of the integrins ($\alpha 2$, $\alpha 3$, and $\alpha 5$) to their respective antibodies (Fig. 6), and hence, it can be suggested that MUC4 interferes with the integrin-mediated cell adhesion by restricting their accessibility to the ligands. A similar observation has also been

reported for SMC/Muc4 (16). Transfection of A375 human melanoma cells with SMC resulted in a significant reduction of cell-cell and cell-matrix interactions. Furthermore, the extent of interference was directly correlated with the size of the tandem repeat domain (16). Similar results have been documented for MUC1 by overexpressing it in transformed epithelial and cancer cell lines (33).

An altered expression of genes is observed in response to *MUC4* down-regulation (Tables 1 and 2). Among the various growth- and metastasis-associated genes up-regulated in *MUC4*- overexpressing cells are *LI-cadherin, CEACAM6, tumor-associated calcium signal transducer-2, AnnexinA1, thrombomodulin, epiregulin, S100A4*, and *macrophage inhibitory cytokine 1* (34-36). An up-regulation of *LI-cadherin* has been shown to correlate with lymph node metastasis in gastric cancer (37, 38). Lymph node is one of the most metastasized sites in pancreatic cancer. *CEACAM6* expression is correlated with a poor survival in pancreatic cancer patients (39). Furthermore, silencing of *CEACAM6* expression by using siRNA in pancreatic adenocarcinoma cells suppresses anoikis resistance *in vitro* and metastatic ability *in vivo* (40). An overexpression of *AnnexinA1*, a Ca^{2+}-dependent phospholipid binding protein, in pancreatic adenocarcinoma is correlated with differentiation of cancer cells during tumorigenesis (41). It has previously been identified as being significantly up-regulated in pancreatic head adenocarcinomas by cDNA microarray analysis (42). MUC4 also up-regulated the expression of Dynein, a protein associated with the retrograde organelle transport and some aspects of mitosis, and Sec61, which is associated with protein transport (43). An up-regulation of the *NCK-associated protein 1,* RAC1, ARP2/3 protein complex subunit p21 (*ARC21*), and *ARP1* was also reported in the *MUC4*-overexpressing cells when compared with the *MUC4*-knockdown cells. All these proteins are key regulators of cell motility (44), which was significantly higher in *MUC4*-overexpressing cells compared with *MUC4*-knockdown cells. RAC1 and NCK are known to stimulate DNA synthesis in the presence of fibroblast growth factor-2 via activation of c-Jun NH_2-terminal kinase pathway (45). Hence, the RAC1 and NCK protein networks might be indirectly responsible for the MUC4-mediated induction of cell proliferation.

MUC4-associated changes in gene expression indicate its important role in cell signaling. Transmembrane mucins are hypothesized to serve as sensors of the external environment either through extracellular domain-mediated ligand binding or as a consequence of altered conformations that result from changes in the external biochemical conditions (pH, ionic composition, and physical interactions; refs. 1, 46). In addition, they can transduce signals via the posttranslational modifications of their cytoplasmic tails (1, 46). Cytoplasmic tail of MUC1 is phosphorylated by various kinases, including

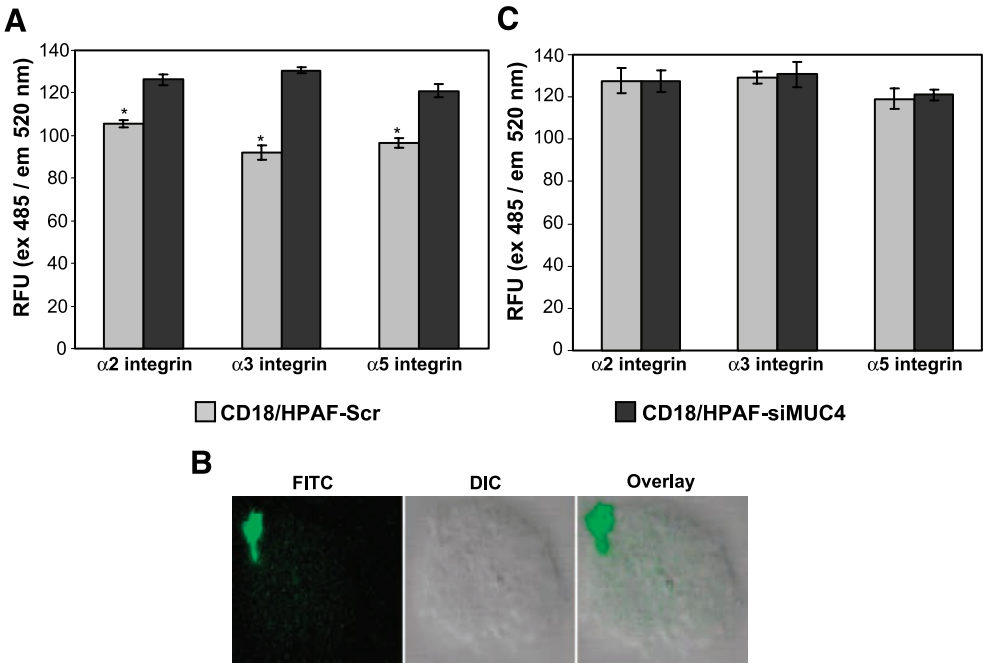

FIGURE 6. Cell surface integrin detection assay. **A.** Cell adhesion to anti-integrin-coated plates. Cells (25×10^3) were seeded in 96-well plate coated with anti-α2, anti-α3, and anti-α5 integrin antibodies. Wells coated with bovine serum albumin served as a negative control. Adhered cells were labeled with calcein-AM and fluorescence was measured at 520 nm after excitation at 485 nm ($n = 3$). *, $P < 0.05$. **B.** MUC4 capping at the cell surface. CD18/HPAF cells in suspension were incubated with FITC-conjugated anti-MUC4 antibody for 1 h at 4°C and washed twice with PBS-Tween 20. After washing, the cells were seeded on coverslips for 1 h at 37°C, fixed in methanol, and mounted on glass slides in antifade mounting medium. Immunostaining was observed under a Zeiss confocal laser-scanning microscope, and representative photographs were captured digitally using 510 LSM software. Magnification, ×100. **C.** Restoration of cell binding to anti-integrin-coated plates after MUC4 capping. MUC4 at the cell surface was capped in CD18/HPAF-Scr and CD18/HPAF-siMUC4 cells as in **B**. After washing, the cells were plated on 96-well plate coated with anti-α2, anti-α3, and anti-α5 integrin antibodies. Wells coated with bovine serum albumin served as a negative control. Adhered cells were labeled with calcein-AM, and fluorescence was measured at 520 nm after excitation at 485 nm ($n = 3$). *, $P < 0.05$.

Table 1. List of Selected Genes Down-Regulated in CD18/HPAF-siMUC4 (*MUC4* Knockdown) Cells Compared with Scrambled siRNA Transfected (CD18/HPAF-Scr)

Gene	Product	Fold Change	Function
SDHC	Succinate dehydrogenase complex, subunit C	4.87	Free radical scavenging
CDH17	Cadherin 17	4.57	Cell adhesion
CEACAM6	Carcinoembryonic antigen-related cell adhesion molecule 6	4.4	Cell adhesion
NCKAP1	NCK-associated protein 1	3.0	Actin assembly
TACSTD2	Tumor-associated calcium signal transducer-2	3.7	Cell surface glycoprotein
ANXA1	AnnexinA1	3.66	Cell signaling
THBD	Thrombomodulin	3.3	Glycoprotein receptor
EREG	Epiregulin	2.9	Growth factor
CLTB	Clathrin, light polypeptide (Lcb)	2.6	Membrane trafficking
S100A4	S100 calcium-binding protein A4	2.6	Calcium-binding protein
PLAB	Prostate differentiation factor	2.5	Growth and differentiation factor
NRG2	Neuregulin-2	2.1	Growth factor
ENPEP	Glutamyl aminopeptidase (aminopeptidase A)	2.4	Cell surface glycoprotein
RAC1	Ras-related C3 botulinum toxin substrate 1	2.27	Cell motility
PPP2CB	Protein phosphatase 2	2.27	Growth-associated protein
PIN	Dynein, cytoplasmic, light polypeptide	2.19	Motor protein
ARC21	ARP2/3 protein complex subunit p21	2.18	Actin polymerization
SEC61G	Sec61 γ	2.1	Protein transport

epidermal growth factor receptor, c-src, glycogen synthase kinase-3β, protein kinase C-δ, Lyn, Lck, and Zap-70, in response to different stimuli. Phosphorylated MUC1 cytoplasmic tail activates different intracellular signaling cascades that can trigger β-catenin-TCF/LEF–dependent, TP53-dependent, or estrogen receptor-α–dependent transcriptional activity and, hence, facilitate tumor progression (47-49). MUC4 has a short cytoplasmic tail (composed of 22 amino acids) that may be engaged in signal transduction and therefore warrants future investigation. Nonetheless, MUC4 may also act as a modulator of cancer cell signaling via disrupting the normal protein-protein interactions and by forming novel, cancer-associated interactions.

In conclusion, our data provide novel evidence supporting the role of MUC4 mucin in the progression of pancreatic cancer. We show that MUC4 sterically regulates the accessibility of cell surface receptors to their ligands. Further, we also show that MUC4 is associated with enhanced cell invasion, altered tumor cell-ECM interaction, and a change in expression of various growth- and metastasis-associated genes. Hence, we propose that MUC4 can be a useful target in the development of novel therapeutic strategies for the treatment of pancreatic cancer.

Materials and Methods

Construction of Plasmid Expressing shRNA against MUC4 and Retroviral Generation

The *MUC4*-specific siRNAs (19 nucleotides) were designed and tested for effective *MUC4* silencing in transient assays. One of the *MUC4* siRNAs (5′-CAGCGACACTAGAGGGACA-3′) located 151 bp downstream of ATG was highly efficient and therefore used for generating a stable shRNA-expressing construct in the pSUPER-retro-puro vector according to the manufacturer's instructions. In brief, two 64-mer oligonucleotides (forward and reverse) containing the 19-bp target sequence in sense and antisense orientation on both sides of the linker TTCAAGAGA were designed. The *Bgl*II and *Hin*dIII restriction sites were located at 5′ and 3′ regions of 64-mers, respectively, to allow direct ligation of the annealed *MUC4* double-strand primer into the pSUPER-retro-puro vector. The annealed double-stranded oligonucleotides were

Table 2. List of Selected Genes Up-Regulated in CD18/HPAF-siMUC4 (*MUC4* Knockdown) Cells Compared with Scrambled siRNA Transfected (CD18/HPAF-Scr)

Gene	Product	Fold Change	Function
SST	Somatostatin	8.2	Growth hormone
DHCR24	Seladin-1	5.4	Senescence protein
DSG2	Desmoglein 2	4.62	Cell junction protein
AP2M1	Adaptor-related protein complex 2	4.52	Vesicular transport
CASP2	Caspase-2	4.5	Proapoptotic protein
DAP	Death-associated protein	4.5	Cell death protein
HMG1	High-mobility group protein 1	4.28	Nuclear protein
CASP3	Caspase-3	4.28	Proapoptotic protein
JUP	Junction plakoglobin	3.2	Cell junction
CDH13	Cadherin 13	2.7	Cell adhesion
TP53BP1	Tumor protein 53-binding protein	2.54	Tumor protein
PIG11	p53-induced protein	2.54	Tumor protein
SMAC	Second mitochondria-derived activator of caspase	2.6	Apoptosis
TP53	Tumor protein p53	2.5	Tumor suppression
CASP7	Caspase-7	2.63	Apoptosis

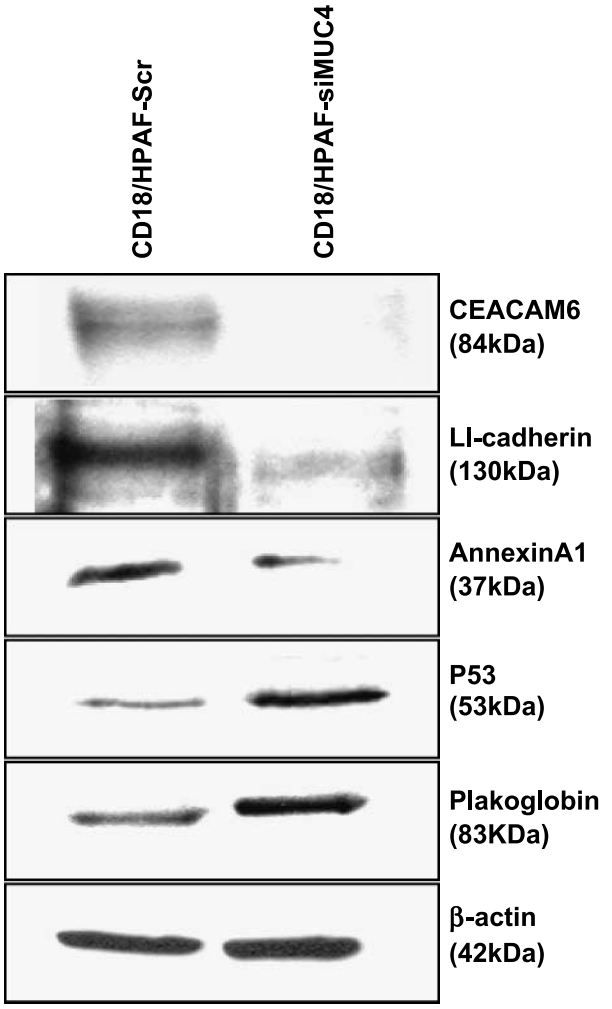

FIGURE 7. Western blot analyses of selected differentially expressed genes (*LI-cadherin, TP53, AnnexinA1*, and *plakoglobin*) identified in microarray. A total of 30 μg protein from cell extracts was resolved by SDS-PAGE, transferred to polyvinylidene difluoride membrane, and probed with respective antibodies. β-actin was used as an internal control. The expression of these genes was in accordance with the microarray data.

phosphorylated using polynucleotide kinase (Roche Diagnostics, Mannheim, Germany) and ligated into the digested pSUPER-retro-puro vector. Successful cloning was ascertained by restriction digestion and sequencing. Ecotropic phoenix packaging cells (gift from Dr. Parmender Mehta, University of Nebraska Medical Center, Omaha, NE) were transfected with the pSUPER-retro-puro vector containing either the MUC4 shRNA insert (pSUPER-retro-puro.siMUC4) or a scrambled sequence (pSUPER-retro-puro.Scr) using LipofectAMINE (Invitrogen, San Diego, CA) following the manufacturer's protocol. Media containing infection-competent retroviruses were collected 48 h after transfection. Polybrene (4 μg/mL) was used to augment the infection efficiency.

Cell Culture and Transfection

CD18/HPAF pancreatic cancer cells were cultured in DMEM supplemented with 10% fetal bovine serum and antibiotics (100 μg/mL of penicillin and streptomycin) at 37°C with 5% CO_2 in a humidified atmosphere. Retroviral supernatants from Phoenix cultures transfected with the pSUPER-retro-puro.siMUC4 or pSUPER-retro-puro.Scr were used for stable transduction of CD18/HPAF cells. Stable clones were then selected in medium containing puromycin (3 μg/mL; InvivoGen, San Diego, CA). The puromycin-resistant colonies were isolated by the ring cloning method and maintained in medium supplemented with puromycin. Medium was replaced with complete medium without antibiotic supplement at least 5 days before any analysis.

Immunoblot and Confocal Immunofluorescence Microscopic Analyses

The CD18/HPAF and derived cell lines were processed for Western blotting and confocal microscopy as described previously (50). In brief, a total of 10 to 30 μg of protein from the cell extracts was resolved by electrophoresis on either a 2.0% SDS-agarose gel (for MUC4) or a 10% SDS-polyacrylamide gel (for other proteins) and transferred to polyvinylidene difluoride membrane. The membrane was probed with anti-MUC4 (1:1,000), anti-TP53 (1:1,000; gift from Dr. Xu Luo, University of Nebraska Medical Center), anti-LI-cadherin (1:1,000; Santa Cruz Biotechnology, Santa Cruz, CA), anti-AnnexinA1 and anti-plakoglobin (1:100; gift from Dr. Keith Johnson, University of Nebraska Medical Center), and anti-β-actin (1:10,000; Sigma, St. Louis, MO) antibodies. The membrane was then incubated with horseradish peroxidase–labeled appropriate secondary immunoglobulin, and the signal was detected using an electrochemiluminescence reagent kit (Amersham Pharmacia, Piscataway, NJ).

For immunofluorescence labeling, cells were grown at low density on sterilized coverslips. After washing with 0.1 mol/L HEPES containing Hanks' buffer, the cells were fixed in ice-cold methanol at −20°C for 2 min. Nonspecific blocking was done with 10% goat serum containing 0.05% Tween 20 for at least 30 min followed by incubation with the anti-MUC4 monoclonal antibody (8G7) in PBS for 90 min at room temperature. Cells were then washed and incubated with FITC-conjugated goat anti-mouse secondary antibodies for 60 min. After washing, the coverslips were mounted on glass slides in antifade Vectashield mounting medium (Vector Laboratories, Burlingame, CA). For actin filament staining, the cells were grown on glass coverslips and fixed with 4% formaldehyde in PBS for 10 min at room temperature. The fixed cells were washed with PBS and permeabilized with 0.2% Triton X-100 in PBS for 5 min. After washing, the cells were stained with Alexa Fluor 488-phalloidin (Molecular Probes, Eugene, OR) for 20 min at room temperature. Cells were washed twice with PBS-Tween 20 and mounted on glass slides in antifade Vectashield mounting medium. Immunostaining was observed under a Zeiss (Carl Zeiss Microimaging, Thornwood, NY) confocal laser-scanning microscope, and representative photographs were captured digitally using the 510 LSM software.

Cell Cycle Analysis

The cells were first synchronized at the G_1-S stage using a double thymidine block. In brief, the cells were treated with

thymidine (Sigma) at 2 mmol/L final concentration for 18 h and washed twice with PBS. The cells were then incubated with fresh medium without thymidine for 9 h at 37°C. The thymidine was added again to a final concentration of 2 mmol/L and incubated for another 18 h and washed with PBS, and fresh medium was added. Following synchronization, the cells were stained with 1 mL propidium iodide (1 μg/mL) and analyzed by flow cytometry.

Apoptosis Assay

Apoptosis was measured by using the Annexin V-FITC apoptosis detection kit (Roche Diagnostics, Indianapolis, IN). The cells were grown in serum-free medium for 72 h. Apoptosis was detected by staining the cells with Annexin V and propidium iodide solution followed by flow cytometry.

Cell Motility Assay

Cells (1×10^6) were plated in the top chamber of noncoated polyethylene terephthalate membranes (six-well insert, pore size of 8 μm; Becton Dickinson, Franklin Lakes, NJ). The bottom chamber contained 1.0 mL DMEM supplemented with 10% fetal bovine serum. The cells were incubated for 24 h at 37°C, and the cells that did not migrate through the pores in the membrane were removed by wiping the membrane with a cotton swab. Cells that passed through the membrane pores were stained with a Diff-Quick cell staining kit (Dade Behring, Inc., Newark, DE). Cells in 10 random fields of view at ×100 magnification were counted and expressed as the average number of cells per field of view. Three independent experiments were done in each case. The data were represented as the average of the three independent experiments.

Cell Invasion Assay

Cells (1×10^5) were seeded on Matrigel-coated membrane inserts (BD Biosciences, Bedford, MA). The bottom chamber contained 0.75 mL DMEM supplemented with 10% fetal bovine serum as a chemoattractant. After incubation for 24 h at 37°C, the cells that remained inside the insert were removed with a cotton swab, and cells that had penetrated the Matrigel to invade to the lower surface of the membrane were fixed in methanol and stained using a Diff-Quick reagent kit. After air drying the membrane, the cells were counted at a magnification of ×100 in 10 random fields of view under a microscope. Assays were done thrice in triplicate.

Cell Adhesion Assay

Cells were harvested and resuspended at a density of 2.5×10^5/mL. A total of 100 μL of the cell suspension (25×10^3 cells) was seeded in triplicate onto the laminin, collagen, fibronectin, and basement membrane complex protein-coated 96-well plates (Calbiochem, La Jolla, CA) and incubated for 1 h at 37°C. After incubation, the cell suspension was discarded and the wells were gently washed twice with PBS. The cells that adhered to the wells were incubated with 100 μL of calcein-AM dye for 1 h at 37°C. The fluorescence of the samples was measured using the fluorescence plate reader at an excitation wavelength of 485 nm and emission wavelength of 520 nm.

Cell Surface Integrin Detection Assay

For the integrin detection assay, goat anti-mouse IgG-coated 96-well plates were incubated with 100 μL of anti-α2, anti-α3, and anti-α5 integrin antibodies (Calbiochem) in separate wells and incubated for 30 min at 37°C. Following incubation, the unbound antibodies were washed off. Cells (25×10^3) were seeded in triplicate in anti-α2, anti-α3, and anti-α5 antibody captured plates and incubated for 1 h at 37°C. After incubation, the cell suspension was discarded and the wells were gently washed twice with PBS. The adhered cells were incubated with 100 μL of calcein-AM dye for 1 h at 37°C. The fluorescence of the samples was measured using the fluorescence plate reader at an excitation wavelength of 485 nm and emission wavelength of 520 nm.

Cell Surface Capping of MUC4

CD18/HPAF cells in suspension were incubated with FITC-conjugated anti-MUC4 antibody (25 μg/mL) for 1 h at 4°C. After washing, the cells were plated on coverslips and incubated for 75 min at 37°C for adherence and fixed in methanol. These cells were then washed twice with PBS-Tween 20 and mounted on glass slides in antifade Vectashield mounting medium. Immunostaining was observed under a Zeiss confocal laser-scanning microscope, and representative photographs were captured digitally.

cDNA Microarray Hybridization and Analysis

RNA (60 μg) from CD18/HPAF-Scr and CD18/HPAF-siMUC4 cell line was fluorescently labeled with Cy3- and Cy5-conjugated dCTP (Amersham Pharmacia) using anchored oligo(dT) primers and SuperScript II reverse transcriptase (Life Technologies, Gaithersburg, MD). After probe generation, residual RNA was hydrolyzed by treatment with NaOH and the unincorporated nucleotides were removed by a MicroCon YM-30 column (Amicon, Billerica, MA). The latter step also served to concentrate the labeled cDNAs. Cy3- and Cy5-labeled cDNAs were combined and diluted to 60 μL with 3.5× SSC/0.15% SDS hybridization solution. To reduce nonspecific hybridization, the hybridization solution also contained 10 μg of poly(deoxyadenylate) (Amersham Pharmacia), 2.5 μg of yeast tRNA (Sigma), and 12.5 μg of human Cot1 DNA (Boehringer-Mannheim, Indianapolis, IN). The fluorescent probes were denatured and hybridized to glass slides featuring ~12,000 oligonucleotides overnight at 65°C. Slides were washed successively in 1× SSC/0.1% SDS, 1× SSC, and 0.2× SSC for 2 min each to remove excess probe. The microarrays were dried by centrifugation for 5 min at 1,000 rpm and scanned immediately with a ScanArray 4000 confocal laser system (Perkin-Elmer, Wellesley, MA). Fluorescent intensity of hybridization signals for each spot was determined automatically and corrected for background. Calculated intensities correlate linearly with the concentration of mRNAs present in the total RNA population because the amount of cDNA attached to the membrane was in excess and the background hybridization signals were sufficiently low. For a quantitative difference in gene expression between arrays, the intensity value of each known gene was normalized in two ways: to the intensity values of the designed housekeeping genes and to the

sum of the intensity values of all of the genes. We found no significant difference in the normalization coefficients generated by the two methods. Comparison of two cell lines (CD18/HPAF-Scr and CD18/HPAF-siMUC4) RNA population was done in two separate parallel hybridization experiments. Genes that showed an average induction or reduction of ≥2-fold in both hybridization experiments were considered to be differentially expressed. Correlations and differences in gene expression between CD18/HPAF-Scr and CD18/HPAF-siMUC4 cells were also compared by scatter plot analysis, in which each point represents a particular gene.

Statistical Analyses

Mean tumor weight and mean tumor volume were compared between groups using an independent sample *t* test. A *P* value of <0.05 was considered as statistically significant.

Acknowledgments

We thank Erik Moore (University of Nebraska Medical Center) for technical support, the Molecular Biology Core Facility (University of Nebraska Medical Center) for oligonucleotide synthesis and DNA sequencing, the Confocal facility for imaging, the FACS facility for cell sorting, and Kristi L.W. Berger (Eppley Institute) for editorial assistance.

References

1. Hollingsworth MA, Swanson BJ. Mucins in cancer: protection and control of the cell surface. Nat Rev Cancer 2004;4:45–60.

2. Hudson MJ, Stamp GW, Chaudhary KS, et al. Human MUC1 mucin: a potent glandular morphogen. J Pathol 2001;194:373–83.

3. Moniaux N, Andrianifahanana M, Brand RE, Batra SK. Multiple roles of mucins in pancreatic cancer, a lethal and challenging malignancy. Br J Cancer 2004;91:1633–8.

4. Buisine MP, Devisme L, Degand P, et al. Developmental mucin gene expression in the gastroduodenal tract and accessory digestive glands. II. Duodenum and liver, gallbladder, and pancreas. J Histochem Cytochem 2000;48:1667–76.

5. Buisine MP, Devisme L, Copin MC, et al. Developmental mucin gene expression in the human respiratory tract. Am J Respir Cell Mol Biol 1999;20:209–18.

6. Swartz MJ, Batra SK, Varshney GC, et al. MUC4 expression increases progressively in pancreatic intraepithelial neoplasia. Am J Clin Pathol 2002;117:791–6.

7. Andrianifahanana M, Moniaux N, Schmied BM, et al. Mucin (MUC) gene expression in human pancreatic adenocarcinoma and chronic pancreatitis: a potential role of MUC4 as a tumor marker of diagnostic significance. Clin Cancer Res 2001;7:4033–40.

8. Iacobuzio-Donahue CA, Ashfaq R, Maitra A, et al. Highly expressed genes in pancreatic ductal adenocarcinomas: a comprehensive characterization and comparison of the transcription profiles obtained from three major technologies. Cancer Res 2003;63:8614–22.

9. Park HU, Kim JW, Kim GE, et al. Aberrant expression of MUC3 and MUC4 membrane-associated mucins and sialyl Le(x) antigen in pancreatic intraepithelial neoplasia. Pancreas 2003;26:e48–54.

10. Jhala N, Jhala D, Vickers SM, et al. Biomarkers in diagnosis of pancreatic carcinoma in fine-needle aspirates: a translational research application. Am J Clin Pathol 2006;126:572–9.

11. Singh AP, Moniaux N, Chauhan SC, Meza JL, Batra SK. Inhibition of MUC4 expression suppresses pancreatic tumor cell growth and metastasis. Cancer Res 2004;64:622–30.

12. Saitou M, Goto M, Horinouchi M, et al. MUC4 expression is a novel prognostic factor in patients with invasive ductal carcinoma of the pancreas. J Clin Pathol 2005;58:845–52.

13. Moniaux N, Nollet S, Porchet N, Degand P, Laine A, Aubert JP. Complete sequence of the human mucin MUC4: a putative cell membrane-associated mucin. Biochem J 1999;338:325–33.

14. Escande F, Lemaitre L, Moniaux N, Batra SK, Aubert JP, Buisine MP. Genomic organization of MUC4 mucin gene. Towards the characterization of splice variants. Eur J Biochem 2002;269:3637–44.

15. Choudhury A, Moniaux N, Winpenny JP, Hollingsworth MA, Aubert JP, Batra SK. Human MUC4 mucin cDNA and its variants in pancreatic carcinoma. J Biochem 2000;128:233–43.

16. Komatsu M, Carraway CA, Fregien NL, Carraway KL. Reversible disruption of cell-matrix and cell-cell interactions by overexpression of sialomucin complex. J Biol Chem 1997;272:33245–54.

17. Price-Schiavi SA, Andrechek E, Idris N, et al. Expression, location, and interactions of ErbB2 and its intramembrane ligand Muc4 (sialomucin complex) in rat mammary gland during pregnancy. J Cell Physiol 2005;203:44–53.

18. Komatsu M, Jepson S, Arango ME, Carothers Carraway CA, Carraway KL. Muc4/sialomucin complex, an intramembrane modulator of ErbB2/HER2/Neu, potentiates primary tumor growth and suppresses apoptosis in a xenotransplanted tumor. Oncogene 2001;20:461–70.

19. Komatsu M, Tatum L, Altman NH, Carothers Carraway CA, Carraway KL. Potentiation of metastasis by cell surface sialomucin complex (rat MUC4), a multifunctional anti-adhesive glycoprotein. Int J Cancer 2000;87:480–6.

20. Carraway KL, Ramsauer VP, Haq B, Carothers Carraway CA. Cell signaling through membrane mucins. Bioessays 2003;25:66–71.

21. Carraway KL, Price-Schiavi SA, Komatsu M, et al. Multiple facets of sialomucin complex/MUC4, a membrane mucin and erbb2 ligand, in tumors and tissues (Y2K update). Front Biosci 2000;5:D95–107.

22. Yamaguchi H, Wyckoff J, Condeelis J. Cell migration in tumors. Curr Opin Cell Biol 2005;17:559–64.

23. Yamazaki D, Kurisu S, Takenawa T. Regulation of cancer cell motility through actin reorganization. Cancer Sci 2005;96:379–86.

24. McGough A, Pope B, Chiu W, Weeds A. Cofilin changes the twist of F-actin: implications for actin filament dynamics and cellular function. J Cell Biol 1997;138:771–81.

25. ffrench-Constant C, Colognato H. Integrins: versatile integrators of extracellular signals. Trends Cell Biol 2004;14:678–86.

26. Semenza GL. VHL and p53: tumor suppressors team up to prevent cancer. Mol Cell 2006;22:437–9.

27. Liang XQ, Cao EH, Zhang Y, Qin JF. P53-induced gene 11 (PIG11) involved in arsenic trioxide-induced apoptosis in human gastric cancer MGC-803 cells. Oncol Rep 2003;10:1265–9.

28. Wen Y, Yan DH, Wang B, et al. p202, an interferon-inducible protein, mediates multiple antitumor activities in human pancreatic cancer xenograft models. Cancer Res 2001;61:7142–7.

29. Chai J, Du C, Wu JW, Kyin S, Wang X, Shi Y. Structural and biochemical basis of apoptotic activation by Smac/DIABLO. Nature 2000;406:855–62.

30. Hanahan D, Weinberg RA. The hallmarks of cancer. Cell 2000;100:57–70.

31. D'Souza-Schorey C. Disassembling adherens junctions: breaking up is hard to do. Trends Cell Biol 2005;15:19–26.

32. Arnaout MA, Mahalingam B, Xiong JP. Integrin structure, allostery, and bidirectional signaling. Annu Rev Cell Dev Biol 2005;21:381–410.

33. Wesseling J, van der Valk SW, Vos HL, Sonnenberg A, Hilkens J. Episialin (MUC1) overexpression inhibits integrin-mediated cell adhesion to extracellular matrix components. J Cell Biol 1995;129:255–65.

34. Koopmann J, Buckhaults P, Brown DA, et al. Serum macrophage inhibitory cytokine 1 as a marker of pancreatic and other periampullary cancers. Clin Cancer Res 2004;10:2386–92.

35. Kluger HM, Kluger Y, Gilmore-Hebert M, et al. cDNA microarray analysis of invasive and tumorigenic phenotypes in a breast cancer model. Lab Invest 2004;84:320–31.

36. Guzman-Aranguez A, Olmo N, Turnay J, et al. Differentiation of human colon adenocarcinoma cells alters the expression and intracellular localization of annexins A1, A2, and A5. J Cell Biochem 2005;94:178–93.

37. Ko S, Chu KM, Luk JM, et al. Overexpression of LI-cadherin in gastric cancer is associated with lymph node metastasis. Biochem Biophys Res Commun 2004;319:562–8.

38. Grotzinger C, Kneifel J, Patschan D, et al. LI-cadherin: a marker of gastric metaplasia and neoplasia. Gut 2001;49:73–81.

39. Duxbury MS, Matros E, Clancy T, et al. CEACAM6 is a novel biomarker in pancreatic adenocarcinoma and PanIN lesions. Ann Surg 2005;241:491–6.

40. Duxbury MS, Ito H, Zinner MJ, Ashley SW, Whang EE. CEACAM6 gene silencing impairs anoikis resistance and *in vivo* metastatic ability of pancreatic adenocarcinoma cells. Oncogene 2004;23:465–73.

41. Bai XF, Ni XG, Zhao P, et al. Overexpression of annexin 1 in pancreatic cancer and its clinical significance. World J Gastroenterol 2004;10:1466–70.

42. Jin G, Hu XG, Ying K, et al. Discovery and analysis of pancreatic

adenocarcinoma genes using cDNA microarrays. World J Gastroenterol 2005;11:6543–8.

43. Bull JH, Ellison G, Patel A, et al. Identification of potential diagnostic markers of prostate cancer and prostatic intraepithelial neoplasia using cDNA microarray. Br J Cancer 2001;84:1512–9.

44. Yamaguchi H, Condeelis J. Regulation of the actin cytoskeleton in cancer cell migration and invasion. Biochim Biophys Acta. In press 2006.

45. Liu JF, Chevet E, Kebache S, et al. Functional Rac-1 and Nck signaling networks are required for FGF-2-induced DNA synthesis in MCF-7 cells. Oncogene 1999;18:6425–33.

46. Singh PK, Hollingsworth MA. Cell surface-associated mucins in signal transduction. Trends Cell Biol 2006;16:467–76.

47. Wei X, Xu H, Kufe D. Human MUC1 oncoprotein regulates p53-responsive gene transcription in the genotoxic stress response. Cancer Cell 2005;7:167–78.

48. Wei X, Xu H, Kufe D. MUC1 oncoprotein stabilizes and activates estrogen receptor α. Mol Cell 2006;21:295–305.

49. Schroeder JA, Adriance MC, Thompson MC, Camenisch TD, Gendler SJ. MUC1 alters β-catenin-dependent tumor formation and promotes cellular invasion. Oncogene 2003;22:1324–32.

50. Moniaux N, Varshney GC, Chauhan SC, et al. Generation and characterization of anti-MUC4 monoclonal antibodies reactive with normal and cancer cells in humans. J Histochem Cytochem 2004;52:253–61.

51. Maina EN, Morris MR, Zatyka M, et al. Identification of novel VHL target genes and relationship to hypoxic response pathways. Oncogene 2005;24:4549–58.

52. Singh AP, Chauhan SC, Bafna S, et al. Aberrant expression of transmembrane mucins, MUC1 and MUC4, in human prostate carcinomas. Prostate 2006;66:421–9.